Crystallization of Silver Chloride in Crazed Porous Polymers

Elena S. Trofimchuk,* Nina I. Nikonorova,* Alexey O. Chagarovskii, Alexander L. Volynskii, and Nikolay F. Bakeev

Department of Chemistry, Moscow State University, Moscow 119992, Russia

Received: April 13, 2005; In Final Form: June 17, 2005

During this study the formation and growth of silver chloride crystals in crazed porous polymeric matrixes of poly(ethylene terephthalate) (PET) and polypropylene (PP) were under investigation. The rate of formation and dispersity and the way AgCl particles aggregate in porous polymers were shown to be dependent on the effective volume porosity, pore dimension, and physical state of the polymer. Methods of the determination of diffusion and distribution constants for low-molecular substances in porous polymers were suggested, and a mechanism of silver chloride crystallization in porous medium was proposed.

Introduction

Crystallization of low-molecular substances in porous matrixes is known to possess some peculiarities in comparison with crystallization in free conditions.[1−3] That fact is a result of pore wall influence, which can be both a surface for heterogeneous nucleation and a restriction for growing particles. Peculiarities of new phase development in porous polymers obtained via solvent crazing[4] are connected with the peculiar properties of the labile fibrillar-porous structure of these polymers. Earlier studies of nickel nanoparticle crystallization in crazed polypropylene matrixes[5−7] established a pattern for the preparation of hybrid materials on the basis of polymeric films with a layer of discrete, distributed metal particles. As it turns out, a ratio of reagent diffusion rate at the reaction front and a rate of reduction were the main factors. However, the development of low-molecular components and their stabilization in crazed matrixes remain uncertain.

To establish nucleation, growth, and stabilization mechanisms for low-molecular substances, an exchange reaction of AgCl precipitation in crazed membranes was studied with a help of kinetic, structural, and morphological methods. Preceding investigations studied AgCl nanoparticle formation in various microreactors: microemulsions,[8,9] amorphous SiO_2 matrixes,[10] and porous polymers.[11,12]

In the following investigation, underlying principles of AgCl formation in porous PET and PP matrixes were determined.

Experimental Section

The porous polymer matrixes were obtained from commercial films of semicrystalline isotactic polypropylene, PP ($M_w = 3 \times 10^5$, thickness of 130 μm, $T_g = -8$ °C), and amorphous poly(ethylene terephthalate), PET ($M_w = 3 \times 10^4$, thickness of 110 μm, $T_g = 70$ °C), by uniaxial stretching in the presence of 2-propanol to tensile strains (ϵ) of 50, 250, and 400% at a constant rate of 5 mm/min. The nucleation and the growth of crazes were carried out via classical crazing.[4] Then prepared porous matrixes were held in a 2-propanol−water (1:4) mixture for a day. The effective volume porosity (W) was estimated by measuring increments of the specimen's volume during its deformation in 2-propanol.[13]

Silver chloride was obtained via the exchange reaction between 2-propanol−water (1:4) solutions of silver nitrate ($AgNO_3$) and sodium chloride (NaCl) with a salt concentration of 0.15 mol/L. The reactants were introduced in a polymer matrix using the countercurrent diffusion technique.[5] The reaction time varied from 5 to 60 min. To remove soluble impurities, the AgCl-containing films were washed with distilled water and dried in a strained state at 60 °C to fixed mass. To avoid silver ion reduction upon exposure to light, all manipulations (reacting, washing, and drying) were conducted in the dark. The mass of AgCl sediment in porous polymer films was determined using a gravimetric procedure ($q = m_{AgCl}/m_p$, where m_p is the mass of the initial porous polymeric matrix). The relative error in determination of AgCl was 10−15%.

X-ray diffraction analysis of the specimens was performed with a DRON-3M instrument using Cu Kα ($\lambda = 1.54$ Å) radiation. Reflections were assigned using the structure database JCPDS-ICDD.[14] The average crystallite size (B) was estimated through the Scherrer formula $B = k\lambda/(\beta \cos \theta) - B = k\lambda(\beta \cos \theta)$, where k is instrumental constant, λ is the wavelength, β is defined as $(\beta_{exp}^2 - \beta_0^2)^{1/2}$, where β_{exp} and β_0 are the experimental and instrumental half-widths of diffraction maximums, respectively, and θ is the Bragg reflection angle at the maximum intensity.

The morphology of the composites obtained was examined with a Hitachi S-520 scanning electron microscope. Samples were prepared using the procedure of brittle fracture in liquid nitrogen and decorated with a platinum−palladium alloy. Image processing was performed using FemtoScan software[15] (Advanced Technologies Center, Russia).

In this work, the diffusion constants and distribution constants of silver nitrate in the PET and PP matrixes with $\epsilon = 250\%$ were determined. For determination of distribution constants (K), nonfilled porous polymeric matrixes were held in $AgNO_3$ solutions with different salt concentrations of 0.1, 0.25, and 0.5 mol/L for 2 days. Then the samples obtained were dried in a strained state at 60 °C to fixed mass. The content of silver (q_{Ag}) in these samples was determined using the scanning electron microscope JSM-5300LV (JEOL, Japan) with energy-dispersive X-ray microanalyzer Link ISIS (Oxford Instruments Mi-

* To whom correspondence should be addressed. Leninskie Gory, Moscow 119899, Russia. Tel: +7(095)9391182. Fax: +7(095)9390174. E-mail: elena_trofimchuk@mail.ru; nni@genebee.msu.ru.

10.1021/jp051920c CCC: $30.25
Published on Web 08/05/2005

TABLE 1: Characteristics of Porous PP and PET Matrices Obtained via Solvent Crazing

polymeric matrix	ϵ, %	W, %	d_p, nm	polymeric matrix	ϵ, %	W, %	d_p, nm
PET-50	50	33	12−14	PP-50	50	30	6
PET-250	250	67	12−14	PP-250	250	60	7
PET-400	400	41	4−6	PP-400	400	53	7

croanalysis Group, U.K.) and it was varied from 0.5 to 3.0 wt %. The relative error in the determination of Ag was 30−50%.

The diffusion constants of $AgNO_3$ (D_{AgNO_3}) in the pores of the polymers were determined with the help of Fick's first law

$$J = -D\,\mathrm{d}c/\mathrm{d}x \qquad (1)$$

Here $J = \mathrm{d}c/\mathrm{d}t$ is the flow of ions to the reaction front, and D is the diffusion constant. To obtain the value of $AgNO_3$ flow, the quantity of $AgNO_3$ moles (n_{AgNO_3}) vs the time of the diffusion (t) were plotted. The original method of n_{AgNO_3} determination was suggested. The porous polymer matrix was disposed in the dialysis cell between the $AgNO_3$ solution with the definite salt concentration (half-cell of I), and the pure solvent consisted of a 2-propanol−water (1:4) mixture (half-cell of II). The concentrations of $AgNO_3$ solutions in I half-cell ranged from 0.05 to 0.6 mol/L. The solutions in the half-cells were permanently mixed to prevent diffusion potential formation at the pore/solution boundary. The concentration of the diffusing substance equaled about zero in the II half-cell. The quantity of silver ions diffused through a polymer matrix during 5, 15, 30, 45, and 60 min was found by Folgard's method. Silver ions were precipitated by potassium thiocyanate in the presence of iron alum. An excess of thiocyanate caused the appearance of a red-colored iron thiocyanate complex. When the precipitate changed into a brown shade, the equivalence point was achieved. The relative error in determination of Ag in the solution was 0.5%. The total amount of diffused $AgNO_3$ was estimated as $n_{AgNO_3}(t) = \sum n_{AgNO_3}(t_i)$.

Results and Discussion

Characteristic of the Porous Polymeric Matrixes. The porous structure of polymers obtained via crazing is a labile, superfine system, which is characterized by definite values of effective volume porosity (W) and average pore dimension (d_p). The W and d_p values for the membranes used in the course of this investigation are represented in Table 1. By comparing the values for PET and PP matrixes with equal rates of deformation (ϵ), we may discover that these polymers have similar characteristics. Moreover they show extremum dependency of W vs ϵ, which is typical for polymers obtained via classical crazing.

The membranes used were obtained at different tensile strains and had a different structure and values of W. A typical structure of a porous polymeric membrane ($\epsilon = 50\%$) obtained via classical crazing is represented in Figure 1. This system consists of alternate areas composed of fibrils and pores and areas of block polymer. With increase of tensile strain to 250%, the part of crazed areas increases due to the growth and widening of the crazes that appeared earlier. Such polymers have the highest values of W. At higher tensile strains, a collapse of fibrillar-porous structure takes place. During the collapse, significant structural realignments occur and the width of polymer films diminishes. Thus values of effective volume porosity and specific surface are deceased (Table 1).

Kinetics of AgCl Precipitation in Porous Polymeric Matrixes. Figure 2 shows the dependency of AgCl accumulation (q) from the reaction's duration. Time plots for PET-50 and

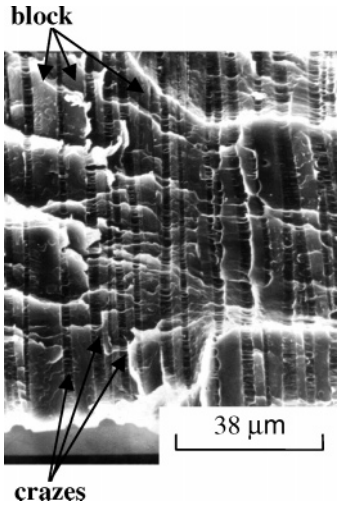

Figure 1. Typical micrograph of a porous polymeric membrane obtained via solvent crazing (PET-50).

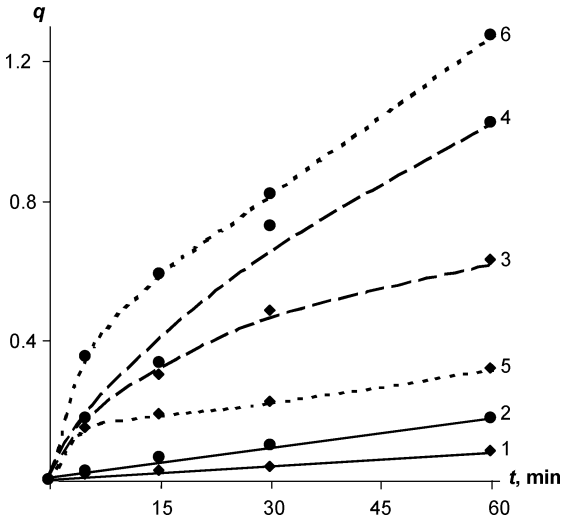

Figure 2. Accumulation curves of AgCl in different PET (1, 3, 5) and PP (2, 4, 6) matrixes, strained in isopropyl alcohol until 50 (1, 2), 250 (3, 4), and 400% (5, 6).

PP-50 tend to be straight lines. For matrixes with a higher tensile strain, graphs show such tendency only at an early stage, then settling velocity decreases. Sedimentation time plots for membranes that differ only in W values show that, during the reaction of AgCl, the precipitation value of the effective porosity is the main factor. It is essential to notice that the settling velocity at late stages ($t > 30$ min) decreases much faster in PET membranes than in PP matrixes.

Differences in the reaction's kinetics observed for PET and PP matrixes which have similar W values might be connected with some peculiarities of diffusion processes in pores of those polymers and with differences in the morphology and lability of polymeric matrixes.

The diffusion rate of the substance in a medium is determined by the initial concentration of a substance and a diffusion constant, which depends on the temperature, medium properties, and nature of the diffusing particle. The following work is dedicated to the determination of diffusion constants D_{AgNO_3} for silver nitrate in crazed polymeric membranes. D_{AgNO_3} values were obtained via the formula

$$D = \frac{Jh_p}{S_p}\frac{1}{Kc_0} \qquad (2)$$

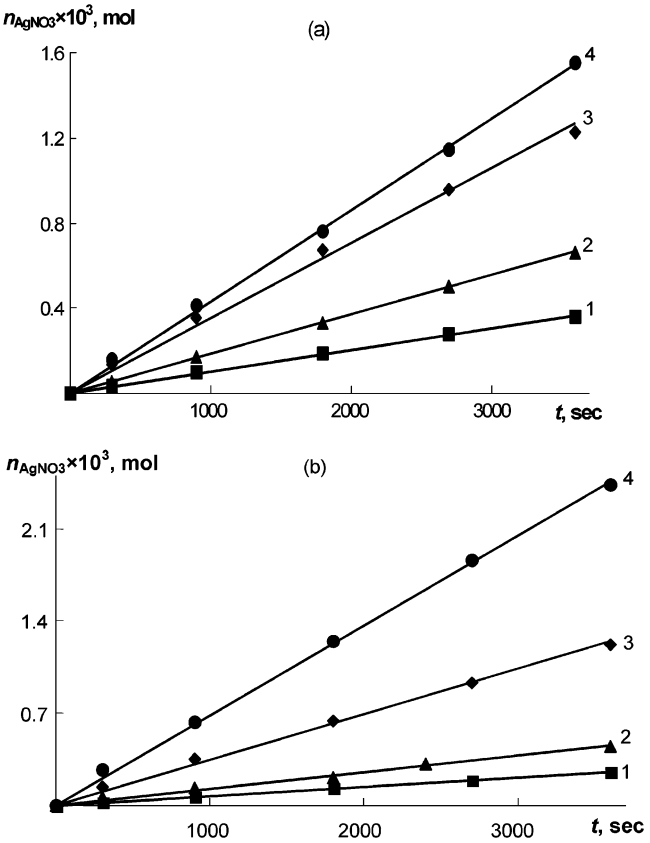

Figure 3. Determination of $AgNO_3$ flow through porous (a) PET-250 (concentrations of initial solutions 0.07 (1), 0.15 (2), 0.28 (3), and 0.49 mol/L (4)) and (b) PP-250 (initial concentrations 0.08 (1), 0.10 (2), 0.40 (3), and 0.60 mol/L (4)) membranes.

which represents Fick's first law (eq 1). Here J is the flow of a low-molecular substance through the membrane, K is a distribution constant of $AgNO_3$ between the reagent's solution and membrane, S_p

$$S_p = \frac{W}{1-W}\frac{V_p}{h_p} = \frac{W}{1-W}\frac{m_p}{\rho_p h_p}$$

(where V_p, m_p, ρ_p, and h_p are the volume, mass, density, and thickness of the polymer, respectively) is the pore area on the surface of the polymeric film, and c_0 is the initial concentration of the $AgNO_3$ solution. Values of thickness were 87 μm for the PET-250 films and 250−90 μm for PP J values were defined as the slope ratio of the corresponding time plots (Figure 3).

A distribution constant K establishes a ratio between the substance concentration in solution and in the pores of the membrane (c_0' (pore) = Kc_0). K values for different polymeric membranes were experimentally measured. The volume of solution in the membrane was considered equal to the pore's volume.

$$K = \frac{c'_0}{c_0} = \frac{1}{c_0}\frac{n_{Ag}}{V} \qquad (3)$$

The n_{Ag} value is a quantity of silver in polymeric film

$$n_{Ag} = \frac{q_{Ag} m_p}{M_{Ag}}, V_p = \frac{W}{1-W} V_p = \frac{W}{1-W}\cdot\frac{m_p}{\rho_p}$$

Here q_{Ag} is an experimentally measured value of the Ag percentage in the film. Thus we can rewrite eq 3 as

$$K = \frac{1}{c_0 M_{Ag}}\frac{q_{Ag}\rho_p(1-W)}{W}$$

The K values for the PET-250 and PP-250 membranes were 0.204 and 0.352, respectively. Relative error was about 50% on account of the poor precision of Ag percentage determination. With the help of determined K values and eq 2, diffusion constants of $AgNO_3$ (D_{AgNO_3}) were calculated for the PET and PP membranes. D_{AgNO_3} values for PET-250 were (2.5 ± 0.5) × 10^{-10} m^2/s and for PP-250 (1.6 ± 0.5) × 10^{-10} m^2/s. In a diluted water solution, values of D_{AgNO_3} are 20−25 times greater—1.76 × 10^{-9} m^2/s. In the crazed membrane, a motion path of diffusing particles is several times greater than the membrane's thickness, because of fibrils and pore branching presence. Thus, values of diffusion velocity for the PET and PP membranes are quite similar (differences in values of diffusion constants are connected with differences in corresponding K values).

Determined values of K and D were used for the theoretical calculation of q_{Ag} values for AgCl sedimentation in porous PET-250 and PP-250 membranes and building corresponding time plots. It is considered a two-stage process: first, a cross-diffusion of reagents takes place (this stage is considered as limitative), then a reaction in the membrane pores occurs.

The product mass after definite time (t) was estimated as

$$m_{AgCl} = \frac{DSKc_0}{l} M_{AgCl} t \qquad (4)$$

Here, M_{AgCl} is the sediment's molar mass, and l is a distance between the surface and reaction front. After making several changes, we may rewrite formula 4 as

$$q = \frac{DKc_0 M_{AgCl} W}{l\rho_p(1-W)h_p} t$$

Within the bounds of the theory used, to calculate q we may need only D and K values for $AgNO_3$ and the reaction's front position. A distance between the surface and reaction front (l) was measured with a scanning electron microscope. l values (60 μm for both samples) were measured relative to the middle of the AgCl layer. The layer's thickness (10 μm for PET-250 and 25 μm for PP-250) was also taken into account. The calculated and experimentally measured time dependencies of Ag content are shown in Figure 4. They show good correlation at early stages. Deviation of experimental data at later stages is connected with decreasing sedimentation velocity as a result of AgCl layer consolidation. Indeed, for porous PP, doping of 50 mass percent of nickel caused a double decrease in permeability.[7] It should be mentioned that deviation for the PET matrix is more significant than that for the PP membrane.

Thus theoretical and experimental data indicate the complexity of AgCl sedimentation in porous polymers, in which the main factor is velocity of diffusion. At an early stage, reaction kinetics is determined only by W values of samples, and for different polymers with similar W values reaction rates are practically equal. Significant differences in the rate of precipitation at later stages might be explained by peculiarities of structure and lability of these polymers. If this supposition is correct, then we may expect the polymer's nature to have an influence on the size of the crystallites and on the processes of crystallite aggregation and distribution in a polymeric matrix.

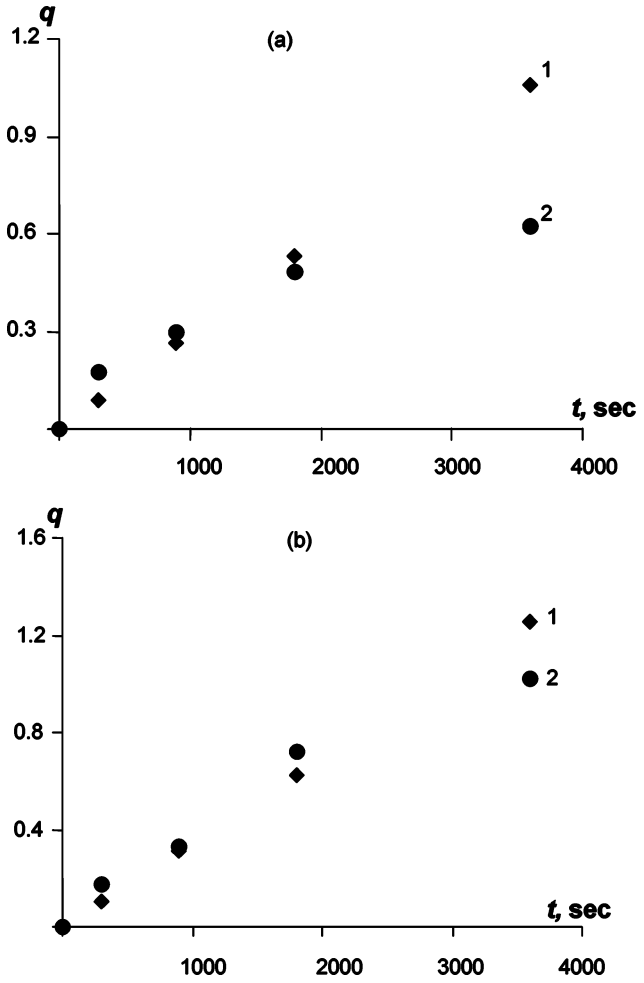

Figure 4. Theoretical (1) and experimentally measured (2) time dependencies of q values for AgCl in (a) PET-250 and (b) PP-250 membranes.

TABLE 2: Structural Parameters of AgCl Crystals in PET and PP Matrices

		B, nm	
ϵ, %	t, min	PET	PP
50	5		85
	15	43	80
	30	33	45
250	5	70	75
	15	23	50
	30	27	85
400	5	25	65
	15	18	55
	30	15	55

Structural Studies of AgCl Crystallization Processes in Porous Matrixes. X-ray diffraction analysis has proved the formation of a AgCl crystalline phase in all polymeric matrixes. Interplanar spacing, which relates to the most intensive signals, was defined with the help of diffraction patterns. Corresponding values were 2.77 Å for plane {200} (d_{litr} = 2.774), 3.20 Å for plane {111} (d_{litr} = 3.203), and 1.96 Å for plane {220} (d_{litr} = 1.962).

Table 2 presents the average size of the AgCl crystallites, which generally does not exceed 85 nm. At the same time, the size of the crystallites that form is at free conditions to 120 nm. In porous PP-250 and PET-250 at early stages (t = 5 min), the average size of the crystallites was 70−80 nm, in PET-400, about 25 nm, and in PET-50, the matrix AgCl crystalline phase was not discovered because of the low content (q < 2 wt %) of substance. At later stages, the average crystallite size depends not only on structural characteristics of membrane but also on the polymer's nature. In PET films after 30 min, crystallite sizes decrease to 20−30 nm, while in the PP matrix, the crystallites remained dimensionally stable (60−80 nm).

It is essential to mention that the average size of the crystallites is greater than the pore sizes. We may suppose that pores differ in sizes and that some pores are large enough to contain crystallites, and growing crystallites move apart flexible fibrils, which connect craze walls.[11] The lability and ability to evolve depend on the physical state of the polymer and the ratio of the fibril's length to its diameter. Greater inflexibility of the PET matrix might be an explanation for smaller (comparing with PP membranes) crystallites.

A decrease of average crystallite size (especially significant for inflexible PET membranes) at later stages may be connected with permanent changes in crystallization conditions, such as reaction volume diminution, changes in supersaturation, and depletion of a favorable place for heterogeneous nucleation. These factors are caused by the formation of smaller or imperfect crystallites.

We may suppose that the main contribution to the process of AgCl formation in porous polymers belongs not to the growth of small crystallites, which formed at an early stage in the reaction, but to the formation of new crystallites, whose dispersity is determined by the lability of the polymer's structure.

Morphological Studies of Polymer−Matrix Composites with AgCl Crystals. Scanning electron microscopy (SEM) investigation of the samples obtained proposed a mechanism for composites forming during new phase precipitation. Figure 5 presents micrographs of polymeric membranes, which contain AgCl crystallites. Comparing empty (Figure 1) and filled polymeric membranes (Figure 5) we may conclude that the structure of the composites obtained via countercurrent diffusion is defined by the structure of the initial matrixes. Composites on the basis of PET-50 are characterized by solid, rodlike blocks of crystallites, about 10 μm in height, which are aligned athwart to the polymer's surface and are localized in separate crazes. An average size of AgCl crystallites in the PET-50 composite does not exceed 43 nm, and linear dimensions of rodlike aggregates are greater and about 1 μm. Thus we may expect these aggregates to consist of nanocrystallites and polymeric fibrils.

To check this supposition, the PET matrix was dissolved in NaOH solution (5 mol/L). Figure 5c shows a micrograph of the particles that remained after dilution. The aggregates seem to be composed of cube crystals. Figure 6 (graph 3) shows the size distribution of particles, with an average size of about 350 nm. Thus, the obtained data are evidence that AgCl rods seen by SEM are not monolithic.

An increase in tensile strain gives rise to the broadening of individual crazes that causes the elongation of AgCl localization areas. In PET-250, aggregates are represented as wide solid bars about 10−15 μm wide and 7 μm in height.

In PET-400, the formation of a practically uninterrupted AgCl layer, which includes solid (∼5 μm) and more friable (∼10 μm) parts, might be observed. This layer consists of single spherical and cubic aggregates about 100−300 nm in diameter. The formation of an uninterrupted layer is connected with the peculiarities of the porous structure of polymers with a high tensile strain.

In PP matrixes, AgCl crystallites form a heterogeneous layer. First, an incompact and interrupted layer, consisting of spherical and cube AgCl aggregates, 200−300 nm in diameter, is formed (Figure 5b). Subsequent AgCl sedimentation in the polymer

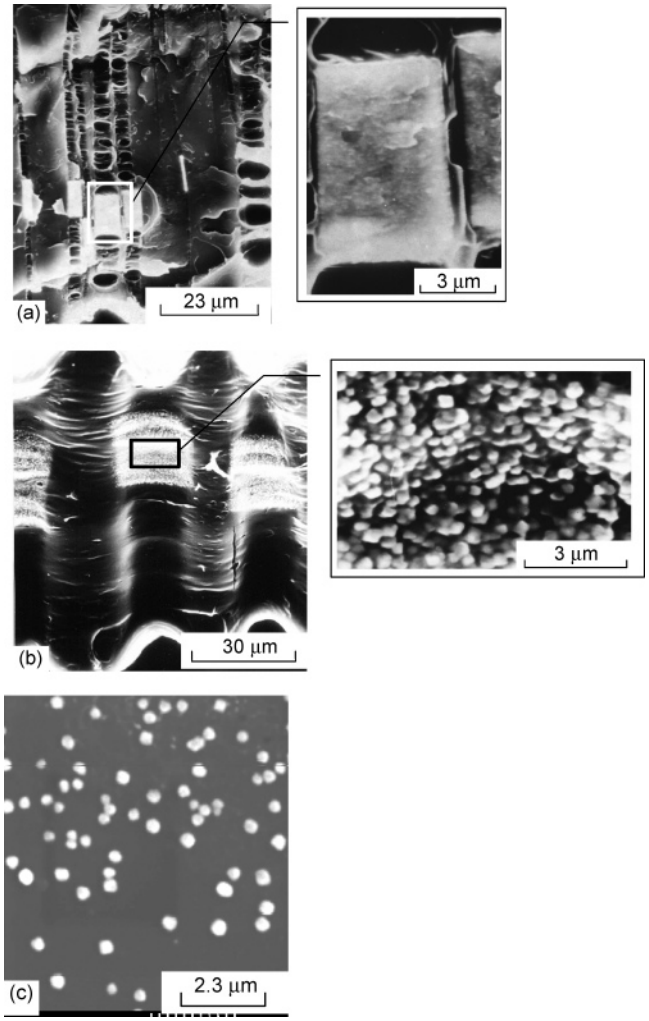

Figure 5. Micrographs of (a) PET and (b) PP, containing AgCl phase, and (c) particles remaining after PET matrix dilution.

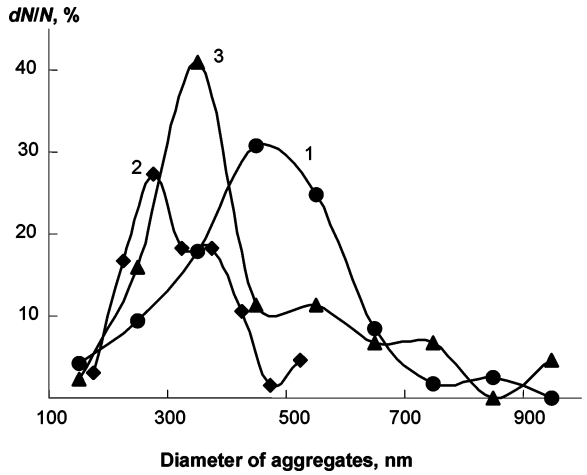

Figure 6. Distribution curves of AgCl aggregates formed at free condition (1), in PP matrix (2), and remaining aggregates after PET matrix dilution (3).

causes enlarging of crystallite-containing areas, which form an uninterrupted layer. That layer has a solid part and a friable part with smaller aggregates. The thickness of the AgCl layer is about 15−40 μm and depends on structure of the initial PP matrix.

Within the bounds of this investigation, size distribution of AgCl aggregates, observed with the help of SEM, was analyzed

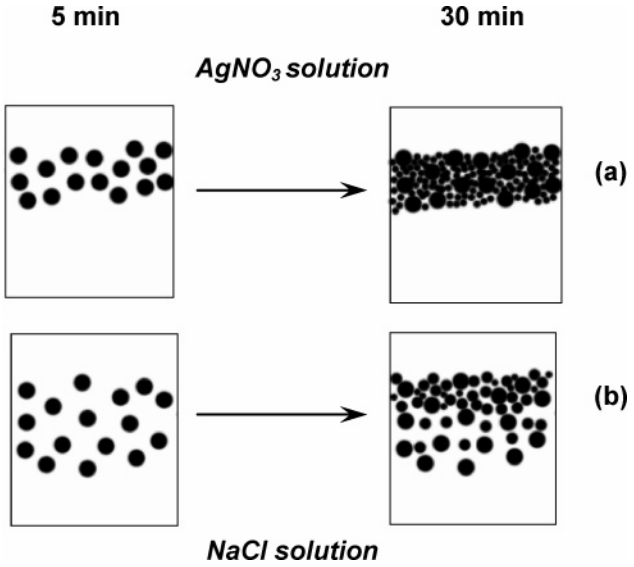

Figure 7. AgCl phase formation scheme for (a) PET and (b) PP matrixes (AgCl particles are marked with black points).

(Figure 6). Curve 1, which refers to distribution of aggregates formed at free conditions, tends to be wide. An average size of the particles is about 500 nm. Execution of the reaction in the PP matrix causes a decrease in the average size down to 250 nm and a restriction of the distribution curve (curve 2).

Conclusions

Thus kinetic, structural, and morphological data allow us to propose a mechanism of AgCl phase formation in porous polymeric medium, represented in Figure 7. At early precipitation stages, the formation of relatively large crystallites takes place. Growth of initial crystallites, obviously, occurs both in large pores and in smaller ones, due to fibril separation. The resulting product accumulation results from the formation of new, smaller crystallites. It is especially well defined for polymer−matrix composites on the basis of PET. Crystallites aggregated into larger particles, involving fibrils in the aggregation process. This fact might be explained by the stabilizing effect of the polymeric matrix during the growth of particles.

The density of layer and presence of polymeric streaks depend on parameters of the porous structure, its lability, and AgCl crystallites dispersity. In the case of PET (Figure 7a), average particle size during crystallization essentially decreases, and smaller crystallites fill up spaces between large crystallites, causing the formation of solid rodlike aggregates. Such a system is almost impermeable for reagents, which results in sedimentation velocity reduction (Figure 2, curve 3). As a result, the formation of a sufficiently narrow layer is observed with the help of SEM. In PP matrixes (Figure 7b), crystallites remain dimensionally stable and form a quite friable heterogeneous layer. That layer remains permeable much longer. Therefore AgCl accumulation proceeds for a longer time (Figure 2, curves 4 and 6), and q values are substantially greater.

Acknowledgment. This work has been financially supported by the Russian Foundation for Basic Research (Project 04-03-08041).

References and Notes

(1) Herron, N.; Wang, Yi.; Eddy, M. M.; Stucky, G. D.; Cox, D. E.; Moller, K.; Bein, T. *J. Am. Chem. Soc.* **1989**, *111*, 530.

(2) Foss, C. A.; Hornyak, G. L.; Stockert, J. A.; Martin, Ch. R. *J. Phys. Chem.* **1994**, *98*, 2963.

(3) Jackson, C. L.; McKenna, G. B. *Chem. Mater*. **1996**, *8*, 2128.

(4) Volynskii, A. L.; Bakeev, N. F. *Solvent Crazing of Polymers*; Elsevier: Amsterdam, The Netherlands, 1995.

(5) Stakhanova, S. V.; Nikonorova, N. I.; Zanegin, V. D.; Lukovkin, G. M.; Volynskii, A. L.; Bakeev, N. F. *Polym. Sci.* **1992**, *34* (2), 175.

(6) Stakhanova, S. V.; Trofimchuk, E. S.; Nikonorova, N. I.; Rebrov, A. V.; Ozerin, A. N.; Volynskii, A. L.; Bakeev, N. F. *Polym. Sci., Ser. A* **1997**, *39* (2), 229.

(7) Nikonorova, N. I.; Stakhanova, S. V.; Volynskii, A. L.; Bakeev, N. F. *Polym. Sci., Ser. A* **1997**, *39* (8), 882.

(8) Bagwe, R. P.; Khilar, K. C. *Langmuir* **1997**, *13*, 6432.

(9) Bagwe, R. P.; Khilar, K. C. *Langmuir* **2000**, *16*, 905.

(10) Zayat, M.; Einot, D.; Reisfeld, R. *J. Sol−Gel Sci. Technol.* **1997**, *10*, 67.

(11) Volynskii, A. L.; Yarysheva, L. M.; Arzhakova, O. V.; Bakeev, N. F. *Vysokomol. Soedin., Ser. A* **1991**, *33* (2), 418.

(12) Volynskii, A. L.; Grokhovskaya, T. E.; Shitov, N. A.; Bakeev, N. F. *Vysokomol. Soedin., Ser. B* **1980**, *22* (7), 483.

(13) Arzhakova, O. V.; Yarysheva, L. M.; Gal'perina, I. B.; Volynskii, A. L.; Bakeev, N. F. *Vysokomol. Soedin., Ser. B* **1989**, *31* (12), 887.

(14) *JCPDS-ICDD Database*; 1995, File 31−1238.

(15) Filonov, A. S.; Gavrilko, D. Yu.; Yaminsky, I. V. *FemtoScan SPM Image Processing Software Manual*; Advanced Technologies Center: Moscow, Russia, 2001. http://www.spm.genebee.msu.su/manual/en/index.html.